

# We are IntechOpen, the world's leading publisher of Open Access books Built by scientists, for scientists

6,900

Open access books available

185,000

International authors and editors

200M

Downloads

Our authors are among the

154

Countries delivered to

TOP 1%

most cited scientists

12.2%

Contributors from top 500 universities



WEB OF SCIENCE™

Selection of our books indexed in the Book Citation Index  
in Web of Science™ Core Collection (BKCI)

Interested in publishing with us?  
Contact [book.department@intechopen.com](mailto:book.department@intechopen.com)

Numbers displayed above are based on latest data collected.  
For more information visit [www.intechopen.com](http://www.intechopen.com)



# Convective Transport Characteristics of Nanofluids in Light-Weight Metal Foams with High Porosity

Huijin Xu, Zhanbin Xing, Fuqiang Wang and Changying Zhao

Additional information is available at the end of the chapter

<http://dx.doi.org/10.5772/intechopen.72291>

## Abstract

Metal foams can be well used as ideal materials for various efficient heat transfer devices due to light weight, high specific, and high thermal conductivity. Nanofluids have higher thermal conductivities than traditional fluid, so it can be used as an efficient heat transfer characteristics medium. This paper focuses on heat transfer of nanofluid, metal foam and the combination of the two. The physical properties of nanofluid and metal foam are summarized. The characteristics of flow and heat transfer are introduced. This work creates a close connection between scientific research and practical applications of this dual heat transfer enhancement method.

**Keywords:** metal foam, nanofluid, heat transfer, forced convection, natural convection, phase change

## 1. Introduction

Metal foam owns the advantages of light weight, high specific surface area, high thermal conductivity and relatively high permeability. Owing to recent advances in manufacturing technologies, metal foam becomes commercially available. The metal foam can be well used as an ideal material for manufacturing efficient heat transfer devices: heat exchangers, heat sinks, solar collectors and catalyst reformers. The practical structure of metal foam (copper) is shown in **Figure 1** and the schematic diagram of convective heat transfer through metal foam is shown in **Figure 2**. From **Figures 1** and **2**, the high specific surface area of metal foam, and lots of pores can be found in metal foams. When fluid flowing through metal foam, the high specific surface area can provide a large surface area to the heat transfer. So the metal foam is a very good extended surface of heat transfer. Nanofluid is a special kind of engineered colloids made of a base fluid and nanoparticles (1–100 nm). Nanofluid owns the higher thermal conductivity and single-phase heat transfer coefficient than the base fluid does, so it can be

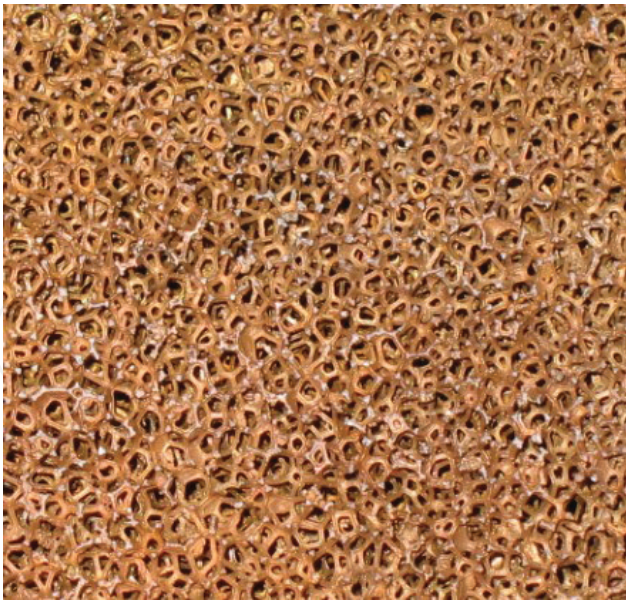


**Figure 1.** The structure of convective heat transfer through metal foams.

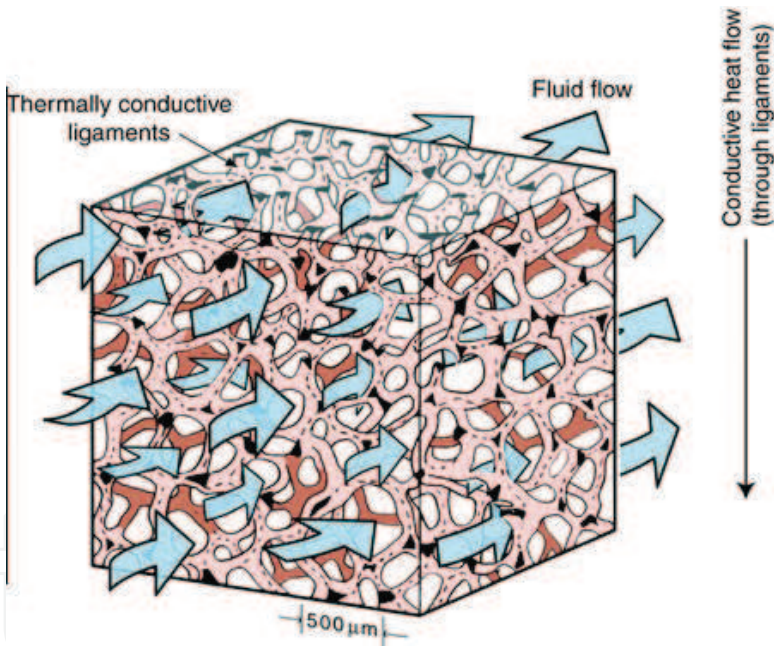


**Figure 2.** The schematic of convective heat transfer through metal foams.

used as an efficient heat transfer medium. The micrograph of the nanofluid is shown in **Figures 3** and **4** shows the schematic diagram of nanoparticles. Nanoparticle is very small and microscopic effects are very obvious. With the addition of nanoparticles, the physical properties of the nanofluid are changed, which made the nanofluid beneficial to heat transfer and attracts widespread attention of scholars. A tremendous number of investigations on the nanofluid can be found in literatures. Furthermore, a lot of experimental researches were conducted on the convective heat transfer of nanofluids, most of which showed that the nanofluid is able to enhance the convective heat transfer. The advantage of the nanofluid and that of the porous foam can be combined as one to further enhance the heat transfer of thermal equipment. For nanofluids flowing through metal foams, some studies have been reported.

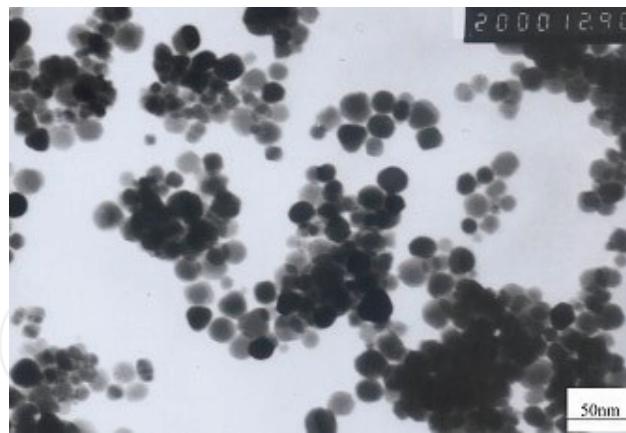


**Figure 3.** Nanofluid.

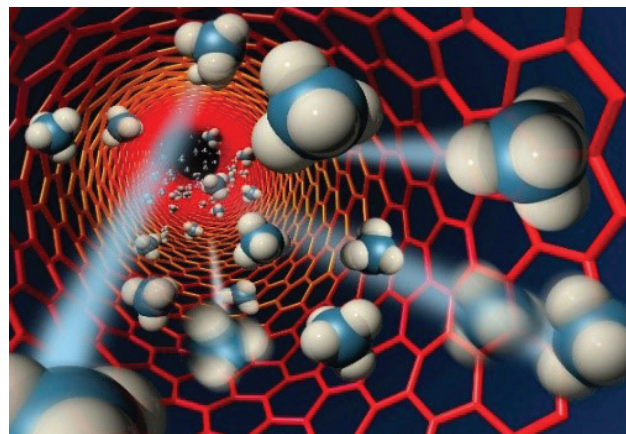


**Figure 4.** Nanoparticles.

In this chapter, flow and thermal transport of nanofluids in metal foams are presented. The recent advances for metal foams, nanofluids, and the combination of nanofluids and metal foams are reviewed. The performance of forced convection, natural convection, and phase change heat transfer of nanofluids in metal foams are analyzed. The contents and the brief introduction for this chapter are shown in the following. Although there is great application potential of nanofluids in thermal science, little attention has been paid to the effect of non-uniform nanoparticle concentration on convective heat transfer of nanofluid in metal foam based on local thermal non-equilibrium (LTNE) model. Hence, laminar convective heat transfer of nanofluid in metal foam with fully developed hydraulic and thermal fields is discussed. The flow and heat transfer characteristics of nanofluids to this case are discussed as well.

## 2. Thermal transport in metal foams

Over the last several decades, flow and heat transfer in metal foam have been studied experimentally, theoretically or numerically by many scholars. In this section, the properties and characteristics of metallic porous media are firstly presented and the recent research progress on thermal transport in porous media is reviewed.



2.1. Pressure drop and permeability

The Darcy model is the first model to describe the percolation theory of porous media. In 1856, Darcy proposed a linear relationship between seepage velocity and pressure drop. Although the theory is simple and easy to understand, but it is very limited. Forchheimer modified the Darcy model by adding the inertia terms associated with the velocity square the equation, but still cannot be applied to the turbulent region. Brinkman considered the effective viscous dissipation term and modified the Darcy model, and found that the results are closer to the molecular diffusion at large porosity [1, 2]. In 1952, Ergun [3] proposed the empirical formula for permeability of porous medium:

$$K = \frac{d_f^2 \varepsilon^3}{150(1 - \varepsilon)^2} \tag{1}$$

In 1998, Calmidi and Mahajan [4] proposed the empirical formula of the metal foam permeability based on the experiment:

$$\frac{K}{d_p^2} = 0.00073(1 - \varepsilon)^{-0.224} \left( \frac{1.18}{1 - e^{-(1-\varepsilon)/0.04}} \sqrt{\frac{1 - \varepsilon}{3\pi}} \right)^{-1.11} \tag{2}$$

Bhattacharya and Mahajan [5] and Plessis et al. [6] proposed an empirical formula of the permeability coefficient and the inertia coefficient by using a foam sample with a pore size of 45–100 PPI and a porosity of 0.973–0.978, and employed water and glycerol as the liquid phase. Many scholars studied the pressure drop and the permeability of the flow in porous media, and the formulas were given in **Table 1**.

2.2. Effective thermal conductivity

The effective thermal conductivity is of great significance for the study of heat transfer mechanism in porous media. Maxwell [10] firstly studied the effective thermal conductivity of

Time	Researcher	Empirical formula	Equation numbers
1994	Plessis et al. [6]	$\frac{K}{d_i^2} = \frac{\varepsilon^2}{36\chi(\chi-1)}, F = \frac{2.05\chi(\chi-1)}{\varepsilon^2(3-\chi)} \cdot \frac{\sqrt{K}}{d_i}$	(3)
2000	Paek et al. [7]	$\frac{\Delta p \sqrt{K}}{L \rho u^2} = f = \frac{1}{Re_\chi} + 0.105 = \frac{\mu}{\rho u \sqrt{K}} + 0.105$	(4)
2006	Liu et al. [8]	$f = 22 \frac{1 - \varepsilon}{Re_{d_p}} + 0.22, 30 < Re_{d_p} < 300$ $f = 0.22, Re_{d_p}$	(5)
2002	Fourie and Plessis [9]	$f_{Fourie} = (3 - \chi)(\chi - 1) \frac{C_D \chi^{1.5}}{24\varepsilon^3}$ $C_D = 1 + (10/Re^{0.667}) = 1 + 10(\rho u d(\chi - 1)/2\mu\varepsilon)^{-0.667}$	(6)

**Table 1.** Models for predicting pressure drop and permeability of flow in porous media.

porous media immersion heat transfer. After that, many scholars studied the effective thermal conductivity of porous media. Most studies of effective thermal conductivity are mainly focused on the volume fraction of each component:

$$k_e = \varepsilon k_f + (1 - \varepsilon)k_s \quad (7)$$

The above model is mainly concentrated on sand, cylindrical, spherical packing bed and fiber insulation blanket, but the estimation of the effective thermal conductivity of metal foam has a large deviation from the experimental result [11]. Calmidi and Mahajan [4] respectively measured the effective thermal conductivity of ERG aluminum foam at the low temperature (ignoring radiation heat transfer) by using air and water as the flow phase. Boomsma and Poulikakos [12] proposed an efficient thermal conductivity model for predicting the three-dimensional ideal cellular structure of metal foam, which is in good agreement with the experimental data of Calmidi and Mahajan [4]. Bhattacharya and Mahajan [5] used the circular cylinder model to modify the Calmidi's correlation. Hadim and North [13] generalized the correlation coefficient of the thermal conductivity model proposed by Wakao et al. [14], and make it applicable to calculate the effective thermal diffusivity and the stagnation thermal conductivity of sintered porous media. The formulas were given in **Table 2**.

Time	Researcher	Empirical formula	Equation numbers
1992	Calmidi and Mahajan [4]	$k_{fe} = \left\{ \frac{2}{\sqrt{3}} \left[ \frac{r(\frac{t}{L})}{k_f + (1+\frac{t}{L})\frac{k_s}{3}} + \frac{(1-r)\frac{t}{L}}{k_f + (\frac{t}{L})\frac{2}{3}(-k_f)} + \frac{\frac{\sqrt{3}-t}{L}}{k_f + (\frac{t}{L})\frac{4r}{3\sqrt{3}}(-k_f)} \right] \right\}^{-1}$	(8)
		$k_{se} = \left\{ \frac{2}{\sqrt{3}} \left[ \frac{r(\frac{t}{L})}{(1+\frac{t}{L})\frac{k_s}{3}} + \frac{(1-r)\frac{t}{L}}{\frac{2}{3}(\frac{t}{L})k_s} + \frac{\frac{\sqrt{3}-t}{L}}{\frac{4r}{3\sqrt{3}}(\frac{t}{L})k_s} \right] \right\}^{-1}$	(9)
		$\frac{b}{L} = \frac{-r + \sqrt{r^2 + \frac{2}{\sqrt{3}}(1-\varepsilon) \left[ 2-r \left( 1 + \frac{4}{\sqrt{3}} \right) \right]}}{\frac{2}{3} \left[ 2-r \left( 1 + \frac{4}{\sqrt{3}} \right) \right]}, r = 0.09$	(10)
		$k_f = \alpha_l k_l + \alpha_v k_v$	(11)
2001	Boomsma and Poulikakos [12]	$\frac{k_{cc}}{k_s} = \frac{1}{\sqrt{2}} \left\{ \frac{4\lambda}{2e^2 + \lambda\pi(1-e)} + \frac{3e-2\lambda}{e^2} + \frac{(\sqrt{2}-2e)^2}{2\pi\lambda^2(1-2e\sqrt{2})} \right\}^{-1}$	(12)
		$e = 0.339, \lambda = \sqrt{\frac{2(2-\frac{5\sqrt{2}}{8}e^3-2e)}{\pi(3-4\sqrt{2}e-e)}}$	
2002	Bhattacharya and Mahajan [5]	$k_{fe} = \left[ \frac{2}{\sqrt{3}} \left( \frac{t/L}{k_f + ((k_s - k_f)/3)} + \frac{\frac{\sqrt{3}-t}{L}}{k_f} \right) \right]^{-1}$	(13)
		$\frac{t}{L} = \frac{-\sqrt{3} - \sqrt{3 + (1-\varepsilon)(\sqrt{3}-5)}}{1 + \frac{1}{\sqrt{3}} - 8/3}$	(14)
1982	Wakao [14]	$(k_e)_x = \varepsilon k_f + (1 - \varepsilon)k_s + 0.5PrRe_d \left( \frac{u}{u_m} \right) k_f$	(15)
		$(k_e)_y = \varepsilon k_f + (1 - \varepsilon)k_s + 0.1PrRe_d \left( \frac{u}{u_m} \right) k_f$	(16)

**Table 2.** Models for predicting effective thermal conductivity of porous media.

### 2.3. Convective heat transfer coefficient

Lu et al. [15, 16] studied the forced convection characteristics of shell-and-tube heat exchangers filled with high porosity metal foams. Qu et al. [17] experimentally studied the natural convection of air in a open-cell copper foam, and found that there is a turning point in the Grashof number for small porosity ( $\varepsilon = 0.9$ ). Guo [18] numerically simulated the laminar forced-convection heat transfer in a porous medium flat plate channel with constant heat flux and analyzed the flow and heat transfer performance. Fand et al. [19] immersed the porous medium in water or silicone oil with the porous medium randomly stacked by glass spheres. Many researchers studied convective heat transfer of flow in porous media, the formulas for predicting Nusselt number were given at **Table 3**.

Because of the difference between the thermal conductivity of the fluid and that of the metal foam, the heat is diffused at a different rate between the two phases. So some researchers hold that the solid and fluid phases have different temperatures, namely LTNE model. Convective heat transfer performance in metal foams was numerically investigated based on the local thermal equilibrium (LTE) model and the LTNE model and the velocity and temperature fields was obtained.

The steady forced convective heat transfer in a tube fully filled with metal foam is numerically considered under the boundary condition of a uniform temperature. Effects of porosity on mean Nusselt number with LTE/LTNE models are shown in **Figure 5**. The LTE and LTNE Nusselt numbers are both decreased with an increase in foam porosity. The relative deviation is reduced by increasing porosity, due to the greatly decreased solid effective thermal resistance. When porosity is greater than 95%, the relative deviation between LTE/LTNE Nusselt numbers is lower than 20%. For  $\varepsilon > 95\%$ , the LTE model can be treated as a rapid estimation tool for thermal performance of metal foams.

Difference between solid and fluid thermal conductivities is the most significant quantity for metal foam LTNE effect. **Figure 6** presents the effects of thermal conductivity ratio on mean Nusselt numbers with LTE/LTNE models. The Nu difference for LTE/LTNE models is reduced when thermal conductivity ratio is increased, which is attributed to that  $k_{fe}/k_{se}$  is increased

Time	Researcher	Empirical formula	Equation numbers
1982	Fand et al. [19]	$NuPr^{0.0877} = 0.618Ra^{0.698} + 8.54 \times 10^6 Ge \times \text{sech}Ra, (0.001 < Re_{max} = 3)$	(17)
		$NuPr^{0.0877} = 0.766Ra^{0.374} \left(\frac{C_1 d}{C_2}\right)^{0.173} (3 < Re_{max} = 100)$	(18)
2003	Boomsma et al. [20]	$Nu = \frac{q}{A_{con}(T_{pl} - T_{c, inlet})} \frac{D_{hyd}}{k_c} = \frac{mc(T_{c, outlet} - T_{c, inlet})}{A_{con}(T_{pl} - T_{c, inlet})} \frac{D_{hyd}}{k_c}$	(19)
2007	Arisetty et al. [21]	$Nu = \frac{2Rh}{k_t} = \frac{2Rq_w}{k_t(T_w - T_{t,b})}$	(20)
2000	Calmidi and Mahajan [22]	$Nu_{sf} = \frac{h_{sf} d_t}{k_t} = C_T Re_{dt}^{0.5} Pr^{0.37} = C_T \left(\frac{V d_t}{\varepsilon v}\right)^{0.5} Pr^{0.37}$	(21)
2005	Brito and Rodríguez [23]	$Nu = 1.1 Re^{0.43} Pr^{1/3}, 10 < Re < 100$	(22)
		$Nu = 1.2 Re^{0.43} Pr^{1/3}, 20 < Re < 240$	(23)

**Table 3.** Models for predicting Nusselt number of heat transfer in porous media.

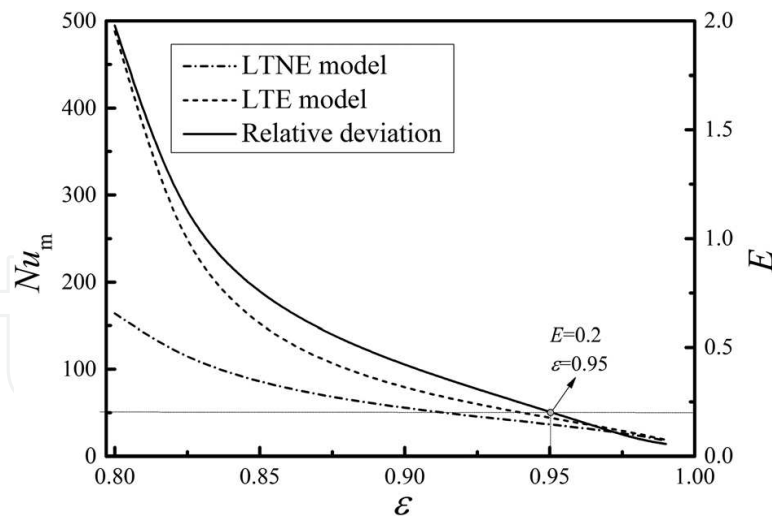


**Figure 5.** Effect of porosity on mean Nusselt number.

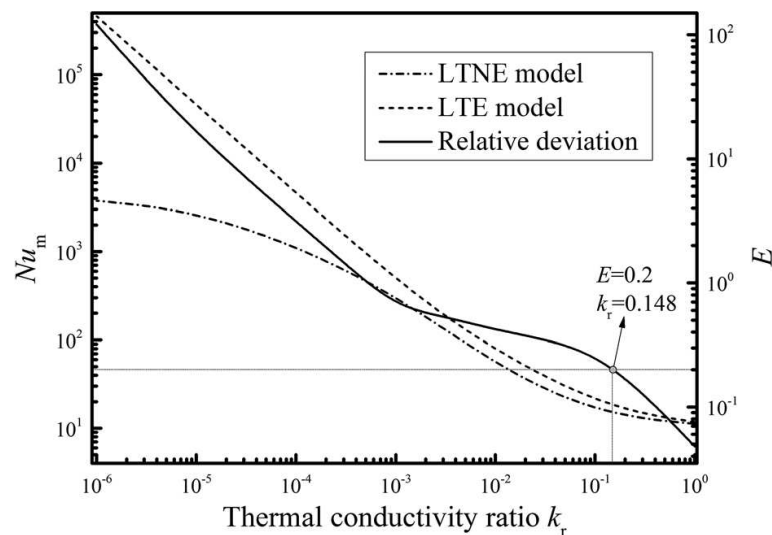


**Figure 6.** Effect of thermal conductivity ratio on mean Nusselt number with LTE/LTNE models.

with an increase in thermal conductivity ratio. When fluid thermal conductivity equals to solid thermal conductivity ( $k_r = 1$ ), LTE Nusselt number coincides with LTNE Nusselt number, in which condition with the LTNE effect is negligible and the LTE assumption holds. In addition, the relative deviation gradually decreases to zero with an increase in thermal conductivity ratio. The relative deviation is reduced to 20% when thermal conductivity ratio is increased to 0.148. The LTE model can be roughly used for prediction of heat transfer in porous foams instead of LTNE model in the range  $k_f/k_s > 0.148$ .

### 3. Transport phenomena in nanofluids

The concept of nanofluid, by adding nanoparticles into a base fluid, is firstly proposed in 1995 [24]. Since then, lots of work has been done on the transport phenomena of nanofluid. In this



work, the basic features of nanofluid are comprehensively presented. Nanofluid is a new type heat exchange medium which is made by mixing highly conductive nanoparticles and the traditional heat transfer fluid. Due to the addition of nanoparticles, the density, the thermal conductivity and the viscosity of nanofluid are obviously different from those of traditional media, and can be used as a more efficient heat exchange medium.

### 3.1. Thermal conductivity

Lee et al. [25] have measured the thermal conductivity of four nanofluids: copper oxide and water, copper oxide and ethylene glycol, alumina and water, alumina and ethylene glycol. Li and Xuan [26] analyzed the mechanisms of nanofluids to improve the thermal conductivity. Xie et al. [27] measured the thermal conductivity of the alumina nanoparticle suspension. The influence of pH value of suspension, specific surface area of the dispersed system, crystallization of solid phase and thermal conductivity of the base fluid on the nanofluid thermal conductivity was studied. Eastman et al. [28] measured the thermal conductivity of the copper nanofluid and found that the thermal conductivity of nanoparticles is increased obviously. Guo [29] used KD-2 thermal analyzer to measure the thermal conductivity of the nanofluid. Using the temperature oscillation technique, Das et al. [30] prove that the thermal conductivity of copper oxide/water and alumina/water increases with an increase in the temperature and a decrease in the particle size. Patel et al. [31] have also obtained similar conclusions through experiments. Ebrahimnia-Bajestan et al. [32] applied nanofluids to the solar system, and studied the laminar convection heat transfer of the  $\text{TiO}_2$ /water nanofluid in a tube by experimental and numerical methods. Many researchers proposed models of nanofluids thermal conductivity base on experimental study [33–47], and the formulas were given in **Table 4**.

### 3.2. Viscosity and friction factor

At present, there is no suitable theory to predict the viscosity of nanofluids accurately. Einstein [48] proved that the relative viscosity of the suspension is a simple function of the volume fraction of suspended particles. Scholars revised the formula in different aspects, and put forward their correction models respectively [39, 49]. With a least-square curve fitting, Maïga et al. [50] proposed a correlation based on some experimental data available in the open literature. Shafahi et al. [51] indicated that the nanofluid viscosity is a function of the temperature and proposed the correlations. Scholars proposed correlations of different nanoparticle types. The formulas of nanofluids viscosity were given in **Table 5**.

Xuan et al. [34, 53] found that the friction factor of nanofluids is almost the same as that of water at the same velocity, and is independent of the volume fraction of nanoparticles. Therefore, the friction factor of nanofluids is calculated with a single-phase model:

$$\lambda_{\text{nf}} = \frac{\Delta P_{\text{nf}} d}{L} \frac{2g}{u_m^2} \quad (24)$$

### 3.3. Convective heat transfer

As a new type heat exchanging medium, the nanofluid has a very pronounced enhancement effect on the convective heat transfer. Scholars have carried out a series of studies on the

Time	Researcher	Empirical formula	Equation numbers
1873	Maxwell [33]	$k_{nf} = \frac{k_{np} + 2k_{bf} + 2(k_{np} - k_{bf})\phi}{k_{np} + 2k_{bf} - (k_{np} - k_{bf})\phi} k_{bf}$	(25)
1999	Lee et al. [25]	$k_{nf} = \frac{k_{np} + (n-1)k_{bf} - (n-1)(k_{bf} - k_{np})\phi}{k_{np} + (n-1)k_{bf} + (k_{bf} - k_{np})\phi} k_{bf}, n = 3/\psi$	(26)
2011	Lee et al. [35]	$\frac{k_{nf}}{k_{bf}} = 1 + 4.4 \left( \frac{T}{T_f} \right)^{10} \left( \frac{k_{np}}{k_{bf}} \right)^{0.03} Pr^{0.66} Re^{0.4}$	(27)
2003	Wang et al. [37]	$k_{nf} = \frac{(1-\phi) + 3\phi \int_0^\infty \frac{k_{cl}(r)n(r)}{k_{cl}(r) + 2k_{bf}} dr}{(1-\phi) + 3\phi \int_0^\infty \frac{k_{cl}(r)n(r)}{k_{cl}(r) + 2k_{bf}} dr} k_{bf}$	(28)
2004	Yu et al. [38]	$k_{nf} = \frac{k_{np} + 2k_{bf} + 2(k_{np} - k_{bf})(1+\beta)^3 \phi}{k_{np} + 2k_{bf} - (k_{np} - k_{bf})(1+\beta)^3 \phi} k_{bf}$	(29)
2013	Hadadian [39]	$\frac{k_{nf}}{k_{bf}} = \frac{k_{np} + 2k_{bf} - 2\phi(k_{bf} - k_{np})}{k_{np} + 2k_{bf} + \phi(k_{bf} - k_{np})} + \frac{\rho_{np}\phi C_{p,np}}{2k_{bf}} \sqrt{\frac{k_B T}{3\pi r_d \mu_{bf}}}$	(30)
2005	Xue and Xu [40]	$\left(1 - \frac{\phi}{\alpha}\right) \frac{k_{nf} - k_{bf}}{2k_{nf} + k_{bf}} + \frac{\phi(k_{nf} - k_{bf})(2k_{lr} + k_{np}) - \alpha(k_{np} - k_{lr})(2k_{lr} + k_{nf})}{\alpha(2k_{nf} + k_{bf})(2k_{lr} + k_{np}) - 2\alpha(k_{np} - k_{lr})(k_{lr} + k_{nf})} = 0, \alpha = \left(\frac{d_{np}}{d_{np} + t}\right)^3$	(31)
2002	Keblinski et al. [42]	$Re_{d_{np}} = \frac{C_{RM} d_{np}}{v}$	(32)
2005	Xue [44]	$k_{nf} = k_{bf} \frac{1 - \phi + 2\phi \frac{k_{np} - k_{bf}}{k_{np} - k_{bf} - I_{T-2k_{bf}}} \frac{k_{bf} + k_{np}}{2k_{bf}}}{1 - \phi + 2\phi \frac{k_{bf}}{k_{np} - k_{bf} - I_{T-2k_{bf}}} \frac{k_{bf} + k_{np}}{2k_{bf}}}$	(33)
2016	Esfe et al. [45]	$\frac{k_{nf}}{k_{bf}} = 0.991 + 0.276T\phi + 77.6\phi^2 + 3641.2T\phi^2 + \frac{0.00217}{\sin(T - \phi)} - 6.01 \times 10^{-6} T^2 - 3647.1T\phi \sin \phi$	(34)
2005	Chon et al. [46]	$\frac{k_{nf}}{k_{bf}} = 1 + 64.7\phi^{0.746} \left(\frac{d_{bf}}{d_{np}}\right)^{0.369} \left(\frac{k_{np}}{k_{bf}}\right)^{0.7476} Pr^{0.9955} Re^{1.2321}$	(35)
2011	Khanafer and Vafai [47]	$\frac{k_{nf}}{k_{bf}} = 1 + 1.011\phi + 2.438\phi \left(\frac{47}{d_{np}}\right) - 0.025\phi \left(\frac{k_{np}}{0.613}\right)$	(36)

**Table 4.** Models for predicting nanofluid thermal conductivity.

Time	Researcher	Empirical formula	Equation numbers
1906	Einstein [48]	$\mu_{nf} = (1 + 2.5\phi)\mu_{bf}$	(37)
2005	Maïga et al. [50]	$\mu_{nf} = (1 + 1.73\phi + 123\phi^2)\mu_{bf}$	(38)
2010	Shafahi et al. [51]	$\begin{aligned} \mu_{nf} &= 2.9 \times 10^{-7} T^2 - 2.0 \times 10^{-4} T + 3.4 \times 10^{-2} \text{ for } \phi = 1\% \\ \mu_{nf} &= 3.4 \times 10^{-7} T^2 - 2.3 \times 10^{-4} T + 3.9 \times 10^{-2} \text{ for } \phi = 4\% \end{aligned}$	(39)
2013	Yang et al. [52]	$\begin{aligned} \mu_{nf} &= \mu_{bf}(1 + 39.11\phi + 533.9\phi^2) \text{ for alumina} \\ \mu_{nf} &= \mu_{bf}(1 + 5.45\phi + 108.2\phi^2) \text{ for titania} \end{aligned}$	(40)

**Table 5.** Models for predicting nanofluid viscosity.

convective heat transfer of nanofluids. Xuan et al. [34, 53] established an experimental system to measure the convective heat transfer coefficient of nanofluid and the laminar flow and turbulent flow friction factors in the channel. In nanofluid, the nanoparticles undergo thermophoretic motion with in the temperature gradient field. Researchers have taken more and more attention to the thermophoretic motion of nanoparticles [54, 55]. For the heating of the side wall in a rectangular channel, Berkovski-Polevikov's coefficients have good agreement with the experimental data with length-width ratio between 1 and 10, and MacGregor-Emery's

coefficient has good agreement with the experimental data with length-width ratio greater than 10 [56]. Maïga et al. [50] considered the influence of the nanoparticle volume fraction and the Reynolds number on the average convective heat transfer coefficient of water-based nanofluid. Sakai et al. [57] improved the Buongiorno model for the convective heat transfer of nanofluids, so that it can be applied to continuity equations, momentum equations and energy equations without the effect of nanoparticle volume fraction distribution. Jia and Wang [58] improved the Eubank-Proctor model and fitted out a coefficient of mixture flow considering natural convection. Yang et al. [59] made two kinds nanofluids using graphite nanoparticles, and measured the laminar-flow convective heat transfer coefficient in a horizontal tube heat exchanger. Formulas for Nusselt number of nanofluids convection were given in **Table 6**.

Buongiorno [60] proposed a mathematical model on the non-uniform volume traction of nanoparticles. He assumed incompressible flow, no chemical reactions, negligible external forces, dilute mixture, negligible viscous dissipation, negligible radiative heat transfer, and LTE between nanoparticles and the base fluid [52, 60].

The forced convective heat transfer of the nanofluid in a plain tube at the full development section was studied by the numerical method. **Figure 7** is the effect of nanoparticle volume fraction on the Nusselt number and  $k_w/k_B$  ( $k_w$  is the thermal conductivity of the wall and  $k_B$  is the average thermal conductivity). It can be seen that the Nusselt number increases at first and then decreases with an increase in the nanoparticle volume fraction, and there is a maximum value of the Nusselt number with a suitable nanoparticle volume fraction. The increase in the nanoparticle volume traction leads to a more uniform velocity, which is beneficial to the convective heat transfer. In addition, the high nanoparticle volume fraction can increase the thermal conductivity, so an increase in the nanoparticle volume traction is beneficial to the convective heat transfer. The ratio of the wall thermal conductivity to the average thermal conductivity decreases with an increase in the nanoparticle volume fraction. When the ratio of  $k_w/k_B$  decreases, the Nusselt number is reduced. The effect of nanoparticle volume traction is

Time	Researcher	Empirical formula	Equation numbers
2000	Xuan and Roetzel [53]	$Nu_{nf} = 0.4328 \left( 1.0 + 11.285 \phi^{0.754} Pe_{np}^{0.218} \right) Re_{nf}^{0.333} Pr_{nf}^{0.4} \text{ for laminar flow}$ $Nu_{nf} = 0.0059 \left( 1.0 + 7.6286 \phi^{0.6886} Pe_{np}^{0.001} \right) Re_{nf}^{0.9238} Pr_{nf}^{0.4} \text{ for turbulent flow}$	(41)
2011	Corcione [56]	$Nu = 0.18 \left( \frac{PrRa}{0.2+Pr} \right)^{0.29} \left( \frac{H}{W} \right)^{0.13}, \quad 1 \leq \frac{H}{W} \leq 2, 10^{-3} \leq Pr \leq 10^5, 10^3 \leq \frac{PrRa}{0.2+Pr} \left( \frac{H}{W} \right)^{-3}$ $Nu = 0.22 \left( \frac{PrRa}{0.2+Pr} \right)^{0.28} \left( \frac{H}{W} \right)^{-0.09}, \quad 2 \leq \frac{H}{W} \leq 10, Pr \leq 10^5, Ra \leq 10^{13}$	(42)
2005	Maïga et al. [50]	$Nu = 0.086 Re^{0.55} Pr^{0.5} \text{ for constant heat flux}$ $Nu = 0.28 Re^{0.35} Pr^{0.36} \text{ for constant wall temperature}$	(43)
2015	Jia and Wang [58]	$Nu_{nf} \left( \frac{\mu_{wnt}}{\mu_{nf}} \right)^{0.14} = 2.11 \left[ Gz_{nf} + 0.574 (Gr_{nf} Pr_{nf} \frac{d}{L})^{0.75} \right]^{1/3}, Gz_{nf} = \frac{d}{L} Re_{nf} Pr_{nf}$	(44)
2005	Yang et al. [59]	$\frac{1}{U} = \frac{1}{h_{nf} \left( \frac{A_i}{A_o} \right)} + \frac{D_o}{2k} \ln \frac{D_o}{D_i} + \frac{1}{h_o} = \frac{A_o \Delta T_{lm}}{Q}$ $\Omega = Nu_{nf} Pr_{nf}^{-1/3} \left( \frac{L}{D} \right)^{1/3} \left( \frac{\mu_{nf}}{\mu_w} \right)^{-0.14}$	(45)

**Table 6.** Models for predicting Nusselt number of nanofluid convective heat transfer.

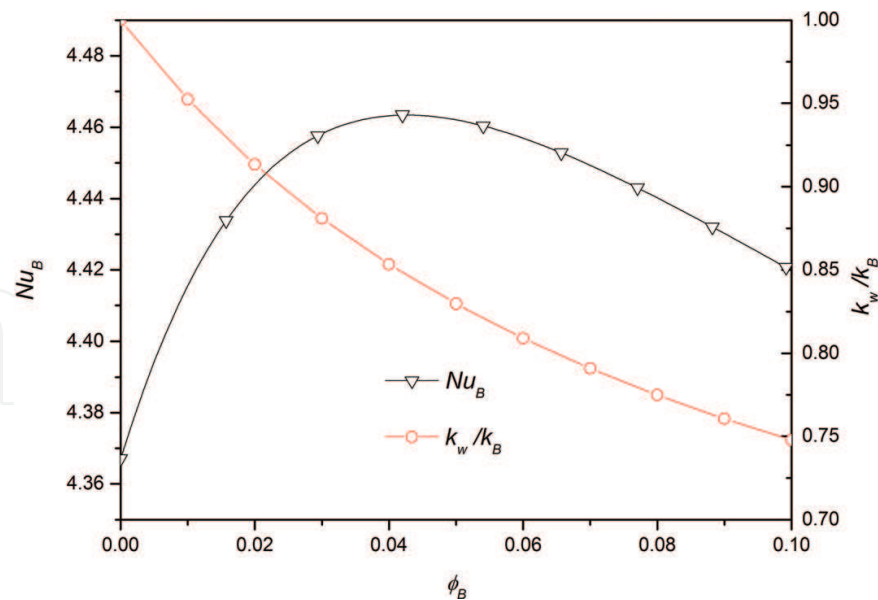


**Figure 7.** Effect of nanoparticle volume fraction on mean Nusselt number.

more obvious with a larger  $k_w/k_B$ , and the effect of  $k_w/k_B$  is more obvious with larger nanoparticle volume traction.

**Figure 8** is the relationship between the Nusselt number and  $N_{BT}$ .  $N_{BT}$  is a dimensionless parameter related to the Brown motion and the thermophoretic motion. It can be found that the nanofluid is unbenefited for heat transfer with low  $N_{BT}$  ( $<0.2$ ). There is a maximum Nusselt number when  $N_{BT}$  is from about 0.4 to 0.5. Then the Nusselt number decreases with an increase in  $N_{BT}$ . When the  $N_{BT}$  is close to 10 or greater, the Nusselt number tends to be constant. The enhancement via the Brown diffusion motion causes nanoparticle to disturb the

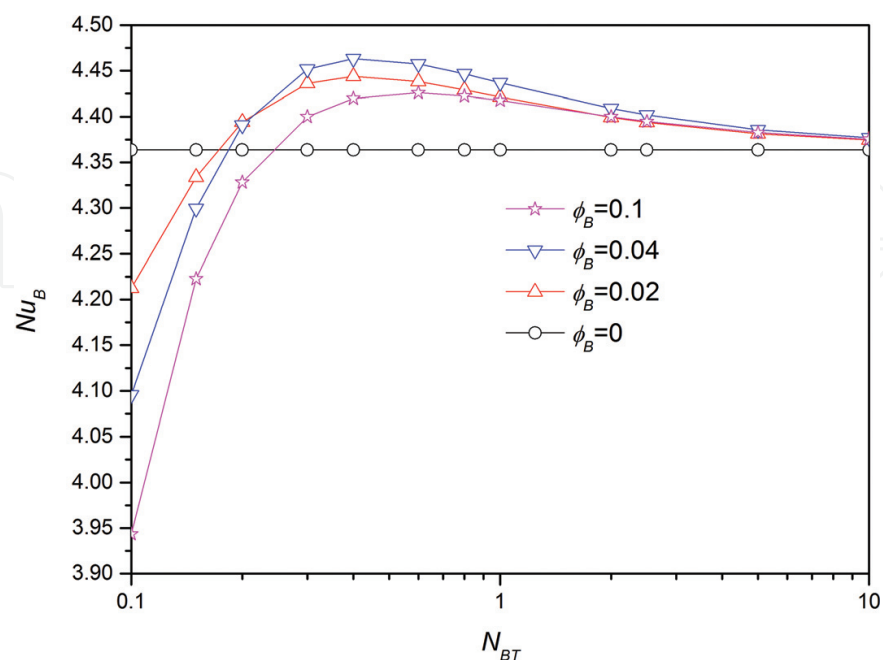


**Figure 8.** Effect of  $N_{BT}$  on mean Nusselt number.

flow more effectively, causing local turbulence to enhance the heat transfer between nanoparticles and the base liquid. Nanoparticles will move to the cold region (wall) by thermophoresis diffusion. For large nanoparticle aggregating, nanoparticle of other areas is too small, so it has little heat transfer enhancement with too large  $N_{BT}$ .

## 4. Convection of nanofluids in metal foams

Even though metal foams own excellent thermal performance, poor heat conduction ability of most heat transfer fluids restricts further heat transfer improvement in metal foams, for which the combination of the metal foam and the nanofluid with highly conductive nanoparticles is a promising solution. In this chapter, the transport characteristics of nanofluids flowing through metal foams. In this chapter, the recent advances on the forced convection and natural convection of nanofluids in porous foams will be firstly reviewed and the latest research concerns from the perspective of fundamental research will be put forward.

### 4.1. Experimental data

Cheng [61] tested the heat transfer performance of the heat pipe with different nanofluid volume fractions and liquid filling rates, and also tested the heat transfer performance of the screen suction core heat pipe. Hajipour et al. [62] studied the mixed convection of alumina/water nanofluid in a vertical square channel partially filled with open metal foams under the constant wall heat flux using the experimental and numerical method. Goodarzi et al. [63] studied the laminar and turbulent mixing flow and heat transfer of Cu/water nanofluids in a shallow rectangular cavity using a two-phase mixture model. Mao [64] studied the generation, fusion and detachment of boiling bubbles on the smooth plate and foam metal surface. Nazari et al. [65] studied the influence of the interaction between nanofluid and porous medium of extended surface on the heat exchanger thermal performance, and the forced convection of alumina/water nanofluids in a circular tube filled with metal foams was studied experimentally with isothermal boundary conditions.

### 4.2. Modeling the forced convective heat transfer

Matin and Pop [66] studied the force convection heat transfer of nanofluids in a horizontal porous medium channel at fully developed section with constant heat flux. Xu et al. [67] investigated the dual heat transfer enhancement of nanofluids flowing in a metal foam channel by numerical method based on the local non thermal equilibrium model. Mahdi et al. [68] summarized the influence of the porosity, permeability, inertial coefficient and effective heat exchange coefficient of porous media, and also studied the effect of thermodynamic parameters of nanofluids. Sivasankaran and Narrein [69] proposed a numerical simulation of laminar pulsating heat transfer and hydraulic characteristics of alumina/water nanofluid in a three-dimensional spiral microchannel radiator, using the modified viscosity equation and the two-phase mixing model.



In Xu et al. [70], velocity and temperature fields are numerically obtained. The effects of some key parameters on flow and heat transfer of nanofluid in porous media are analyzed. For the nanofluid flowing through metal foams, the nanoparticle volume fraction is a most important parameter, the effect of which on pressure drop is shown in **Figure 9**. As can be seen, with the increase in volume fraction, the pressure drop per unit length gradually increases and the increasing amplitude for pressure drop also increases. This is attributed to that the dynamic viscosity and the density of nanofluid are increased sharply with the increase in volume fraction. **Figure 10** shows the effect of nanoparticle volume fraction on heat transfer for two different nanoparticles ( $\text{Al}_2\text{O}_3$  and  $\text{TiO}_3$ ). As the nanoparticle volume fraction increases, Nusselt number gradually increases but the increasing amplitude is reduced. This is attributed to that the thermal conductivity increasing amplitude is decreased with an increase in

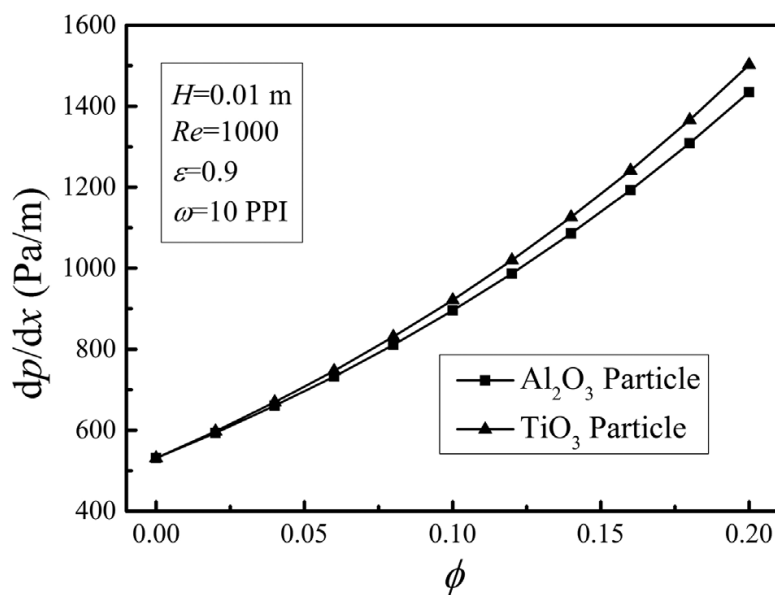


**Figure 9.** Effects of nanoparticle volume fraction on the overall pressure drop.

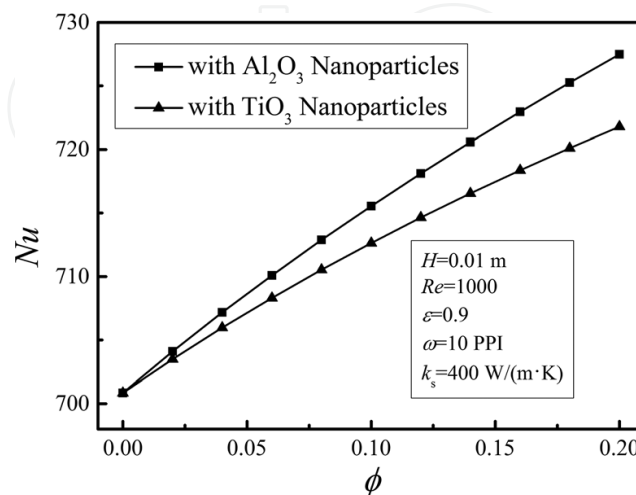


**Figure 10.** Effects of nanoparticle volume fraction on heat transfer.

nanoparticle volume fraction. Due to thermal conductivity of  $\text{Al}_2\text{O}_3$  is higher than that of  $\text{TiO}_3$ , Nusselt number of  $\text{Al}_2\text{O}_3$  is higher than that of  $\text{TiO}_3$  as shown in **Figure 10**. From **Figure 10**, the maximum heat transfer augmentation of nanofluid is about 3.8% for  $\text{Al}_2\text{O}_3$  and 3.0% for  $\text{TiO}_3$ , which is very useful for further improving thermal performance of metal foam heat exchangers and heat sinks, especially for high heat-flux applications.

#### 4.3. Modeling the natural convective heat transfer

Sun and Pop [71] studied the steady natural convection of the water-based nanofluid in a right triangle shell filled a porous medium using the numerical method. It is found that the average Nusselt number can be increased by increasing the nanoparticle volume fraction under a low Rayleigh number, but the average Nusselt number decreases with an increase in the nanoparticle volume fraction under a high Rayleigh number. Sherement [72] established a Buongiorno mathematical model for the three-dimensional natural convection of nanofluids in porous media, and considered that the heterogeneous models of nanoparticles are more suitable. Bhadauria and Agarwal [73] proposed a detailed model of the nanofluid saturated porous layer.

A lattice Boltzmann (LB) model for the nanofluid natural convection in a porous medium was established by using the volume-averaging method. **Figures 11** and **12** show the velocity and temperature distributions for  $Ra = 10^4$  and  $10^6$ , respectively. The other parameters are set to  $Da = 0.0001$ ,  $\varepsilon = 0.6$ , and  $\phi = 0.5\%$ . For  $Ra = 10^4$ , the temperature is very uniform in the y direction, and the heat is transferred mainly by heat conduction. Streamlines are nearly in parallel with the gravitational direction. In **Figure 12**, the high temperature region at the upper left side and the low temperature region the bottom right side respectively diffuse heat with a

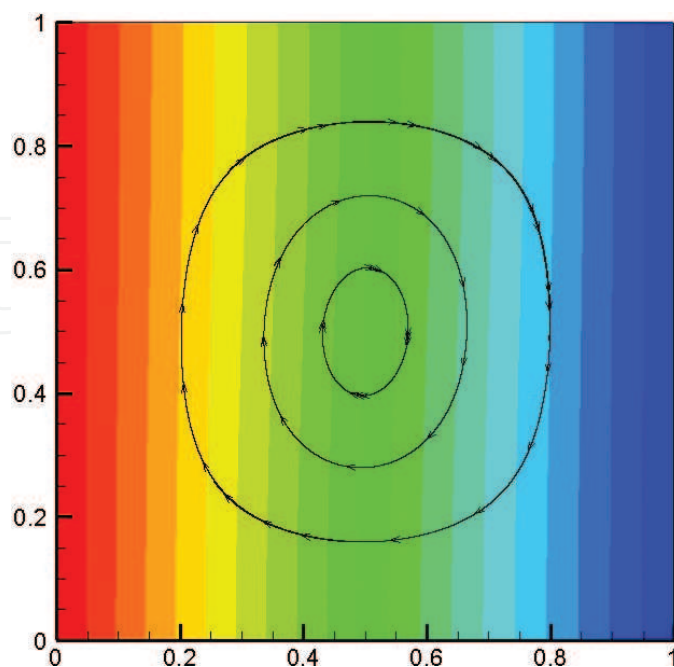


**Figure 11.** The distributions of the flow and the temperature for  $Ra = 10^4$ .

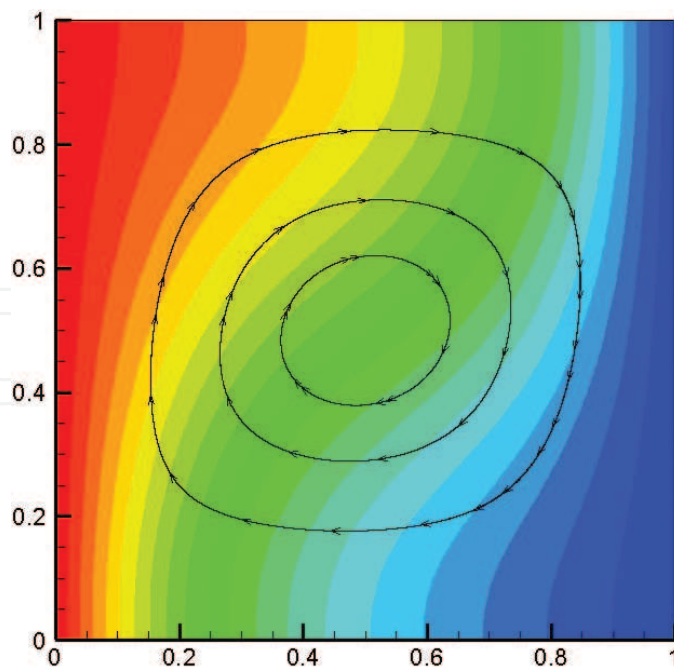


**Figure 12.** The distributions of the flow and the temperature for  $Ra = 10^6$ .

quicker speed than other region. The change of the heat transfer regime from the heat conduction to the natural convection is clearly shown in **Figures 11** and **12**.

**Figure 13** shows the effect of the Rayleigh number on the average Nusselt number with  $Da = 10^{-3}$  and  $Da = 10^{-4}$ . With an increase in the Rayleigh number, the increasing amplitude of  $Nu_{ave}$  is mild for the small Rayleigh number, and  $Nu_{ave}$  increases sharply for large Rayleigh numbers. The effect of  $Ra$  on the flow and  $Nu_{ave}$  is more obvious for the high Darcy number.

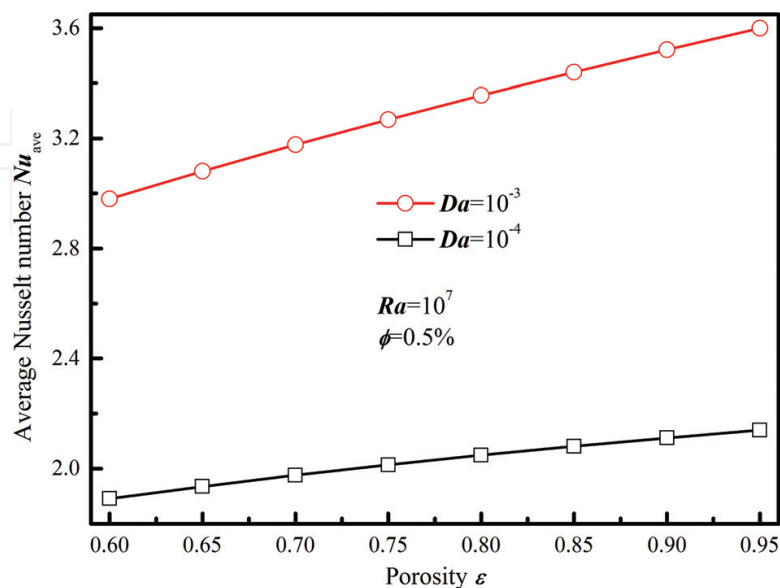


**Figure 13.** Effect of the Rayleigh number on the heat transfer.

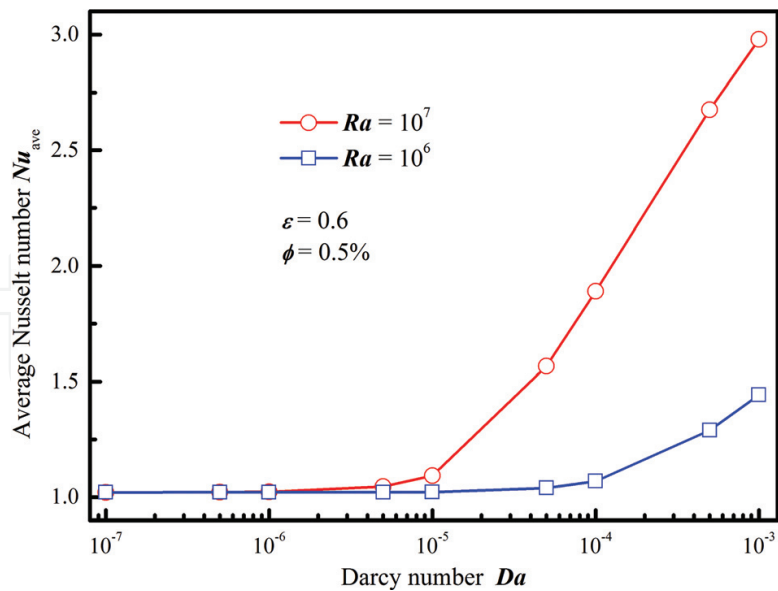


Figure 14. Effect of the Darcy number on the heat transfer.

Figure 14 shows the detailed relationship between the Darcy number and the average Nusselt number. The average Nusselt number almost does not change when  $Da$  is less than  $10^{-5}$ . As  $Da$  increases from  $10^{-7}$  to  $10^{-6}$ ,  $Nu_{ave}$  only increases by 0.03% for  $Ra = 10^6$  and by 0.14% for  $Ra = 10^7$ . Natural convection almost can be ignored and there is only heat conduction when the Darcy number is less than  $10^{-5}$ .

Figure 15 shows the effect of the nanoparticle volume traction on  $Nu_{ave}$  with different thermal conductivities of nanoparticles ( $k_p$ ). Physical characteristics of nanofluids differ for different nanoparticle volume tractions. The thermal conductivity of the nanofluid increases with an

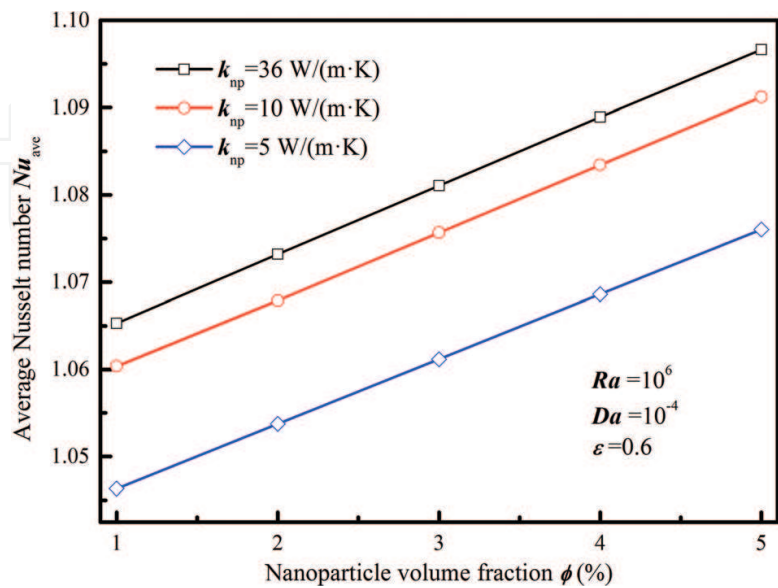


Figure 15. Effect of the nanoparticle concentration on the heat transfer.

increase in the nanoparticle volume traction, and it is beneficial for promoting the heat transfer, which leads to the increased average Nusselt number.

## 5. Phase change heat transfer

Phase change heat transfer of nanofluid in porous foams is a relatively new theme. In this chapter, the basic scientific problems for this topic will be firstly presented and then the recent research advances will be reviewed. The future research points will also be discussed.

### 5.1. Liquid-gas phase change heat transfer

Boiling heat transfer is used in a variety of industrial processes and applications, such as refrigeration, power generation, heat exchangers, cooling of high-power electronics components and cooling of nuclear reactors [74]. The use of nanofluids for boiling heat transfer enhancement is a promising solution that is currently being explored by many researchers for pool boiling applications.

Lee and Mudawar [75] have undertaken an experimental study to explore the benefits of using alumina/water nanofluid for microchannel cooling applications. They revealed the enhancement of the heat transfer coefficient for single-phase laminar flow. However, in the two-phase regime, the nanofluids caused the surface deposition in micro-channels, and large agglomerates of nanoparticles were formed. Kim et al. [76] investigated the subcooled flow boiling using dilute alumina, zinc oxide and diamond water-based nanofluids. Kim et al. [77] studied the pool boiling by experiment with water-based nanofluids containing  $\text{Al}_2\text{O}_3$ ,  $\text{ZrO}_2$  and  $\text{SiO}_2$  nanoparticles. An irregular porous structure was formed at the surface. You et al. [78] measured the CHF in pool boiling using a flat, square copper heater submerged into nanofluids at a sub-atmospheric pressure of 2.89 psia. Nanoparticle deposition was observed by Bang and Chang [79], who also measured a CHF enhancement of 50% with alumina-water nanofluids on a stainless steel plate. Zhu et al. [80] developed a boiling heat transfer coefficient correlation of the refrigerant/lubricating oil mixture on the surface of the metal foam surface.

Several researchers have noticed the nano-deposition at the heater surface, which can alter the surface area, the surface wettability and the bubble nucleation. The nucleation site density, the bubble departure diameter and the bubble frequency are all affected by the nanofluid boiling. It was found by several researchers [77, 78] that bubble diameters increase during boiling with nanofluids, but the nucleation site density decreases with the addition of nanoparticles into the base fluid.

### 5.2. Liquid-solid phase change heat transfer

Liquid-solid phase change in porous media is frequently encountered in lots of natural and engineering systems. Over the past several decades, this problem has been extensively investigated analytically, experimentally and numerically [81]. Thermal management systems based



on latent heat storage of phase change materials (PCMs) can be widely used. Many researches are focused on demonstrating the performance improvement over pure PCM-based thermal management systems and the free and forced-convection heat transfer phenomena inside the porous media [82, 83].

Hong and Herling [84] experimentally studied the effect of surface area density on the performance of paraffin-infiltrated aluminum foams with pore sizes from 500 to 2 mm. Lafdi et al. [85] also conducted an experimental study with paraffin-infiltrated aluminum foams and found that both pore size and porosity affected the performance of the system. Tian and Zhao [86] performed similar experiments with copper foams. With the advancement of fabrication techniques for microcellular metal foams [87], the effect of pore size and porosity becomes more interesting due to the extremely large surface area enabled by metal foams with small pore size. Numerical models were also developed to predict the temperature profile of PCM metal foam systems. These models had an origin in Boomsma and Poulikakos [12], where the effective thermal conductivity ( $k_e$ ) of an infiltrated porous metal foam was estimated based on a tetrakaidecahedron pore model. Tao et al. [88] investigated the latent heat storage (LHS) performance of metal foams/paraffin composite phase change material (CPCM) using lattice Boltzmann method. Gao et al. [89] also used the lattice Boltzmann method to simulate solid-liquid phase change with natural convection in porous media under LTNE conditions.

A new sort of nanofluid phase change material (PCM) is developed by suspending a small amount of nanoparticles in melting paraffin by Wu et al. [90]. Zheng et al. [91] found that Ag/1-Tetradecanol showed remarkably high thermal conductivity and reasonably high phase change enthalpy. Khodadadi et al. [92] numerically simulated the solidification of Cu/H<sub>2</sub>O nanofluids in a vertical square enclosure. Guo [93] numerically obtained that room with alumina/paraffin as PCM ceiling is a good way of saving the required cool energy in summer. Wu et al. [94] investigated the effects of Cu nanoparticles on the thermal conductivity and the phase change heat transfer of Cu/paraffin PCM by the Hot Disk thermal constants analyzer and infrared monitoring methods respectively. The results show that adding nanoparticles is an efficient way to enhance the phase change heat transfer of PCM.

## 6. Summary

Metal foams and nanofluids are greatly potential for the application of practical thermal applications since they are beneficial for heat transfer enhancement. A review of previous study for different convective flow and heat transfer regimes about the metal foam and the nanofluid is presented in this article. The effects of several parameters in metal foam and nanofluid properties, thermal boundary conditions, and flow and heat transfer characteristics were analyzed. Previous studies have shown that nanofluid and metal foam can enhance heat transfer. Some suggestions for future works should be paid attention to, as turbulent flow of nanofluids flow in metal foams, new models for the heat transfer of nanofluids in metal foams, the micro effect of nanofluid, the non-Newtonian effect of nanofluids, and the slip effect of nanofluid in metal foams.

## Acknowledgements

This work is supported by the National Natural Science Foundation of China (No. 51406238), the Fundamental Research Funds for the Central Universities (No. 17CX02047), the Foundation for Outstanding Young Scientist in Shandong Province (No. BS2014NJ009), and the Postdoctoral Science Foundation of China (No. 2015 M570363).

## Author details

Huijin Xu<sup>1,2\*</sup>, Zhanbin Xing<sup>2</sup>, Fuqiang Wang<sup>3</sup> and Changying Zhao<sup>1</sup>

\*Address all correspondence to: [hjxu1015@gmail.com](mailto:hjxu1015@gmail.com)

1 China-UK Low Carbon College, Shanghai Jiao Tong University, Shanghai, China

2 Department of Energy and Power Engineering, College of Pipeline and Civil Engineering, China University of Petroleum (Huadong), Qingdao, China

3 School of Automobile Engineering, Harbin Institute of Technology at Weihai, Weihai, China

## References

- [1] Zheng KC, Wen Z, Wang ZS, Guo-Feng L, Liu XL, Wu WF. Review on forced convection heat transfer in porous media (in Chinese). *Acta Physica Sinica*. 2012;**61**(1):1-11
- [2] Amhalhel G, Furmański P. Problems of modeling flow and heat transfer in porous media. *Biuletyn Instytutu Techniki Ciepłej Politechniki Warsza Wskiej. Journal of Power Technologies*. 1997;**85**:55
- [3] Ergun S. Fluid flow through packed columns. *Chemical Engineering Progress*. 1952;**48**(2): 89-94
- [4] Calmidi VV, Mahajan RL. The effective thermal conductivity of high porosity fibrous metal foams. *Journal of Heat Transfer*. 1992;**121**(2):466-471
- [5] Bhattacharya AC, Mahajan R. Thermophysical properties of high porosity metal foams. *International Communications in Heat and Mass Transfer*. 2002;**45**:1017-1031
- [6] Plessis PD, Montillet A, Comiti J, Legrand J. Pressure drop prediction for flow through high porosity metallic foams. *Chemical Engineering Science*. 1994;**49**:3545-3553
- [7] Paek JW, Kang BH, Kim SY, Hyun JM. Effective thermal conductivity and permeability of aluminum foam materials. *International Journal of Thermophysics*. 2000;**21**(2):453-464
- [8] Liu JF, WT W, Chiu WC, Hsieh WH. Measurement and correlation of friction characteristic of flow through foam matrixes. *Experimental Thermal and Fluid Science*. 2006;**30**(4): 329-336

- [9] Fourie JG, Plessis JPD. Pressure drop modelling in cellular metallic foams. *Chemical Engineering Science*. 2002;**57**(14):2781-2789
- [10] Maxwell JC. *A Treatise on Electricity and Magnetism*. Dover, New York: Oxford University Press; 1954
- [11] Zhao CY. Review on thermal transport in high porosity cellular metal foams with open cells. *International Journal of Heat and Mass Transfer*. 2015;**55**(13):3618-3632
- [12] Boomsma K, Poulikakos D. On the effective thermal conductivity of a three-dimensionally structured fluid-saturated metal foam. *International Journal of Heat and Mass Transfer*. 2001;**44**(4):827-836
- [13] Hadim H, North M. Forced convection in a sintered porous channel with inlet and outlet slots. *International Journal of Thermal Sciences*. 1999;**44**(1):33-42
- [14] Wakao N, Kagei SD. Heat and mass transfer in packed beds. *AIChE Journal*. 1982;**1**(2):193-199
- [15] Lu W, Zhao CY, Tassou SA. Thermal analysis on metal-foam filled heat exchangers. Part I: Metal-foam filled pipes. *International Journal of Heat and Mass Transfer*. 2006;**49**(15):2751-2761
- [16] Zhao CY, Lu W, Tassou SA. Thermal analysis on metal-foam filled heat exchangers. Part II: Tube heat exchangers. *International Journal of Heat and Mass Transfer*. 2006;**49**(15):2762-2770
- [17] Qu ZG, Xu ZG, Tao WQ, Lu TJ. Experimental study of natural convective heat transfer in horizontally-positioned cellular metal foams with open cells (in Chinese). *Journal of Xi'an Jiao Tong University*. 2009;**43**(1):4
- [18] Guo LY. *The Optimal Analysis and Effect of Flow and Heat Transfer in a Parallel-Plate Channel Filled with Porous Media* (in Chinese). Lanzhou: Lanzhou University of Technology; 2013
- [19] Fand RM, Steinberger TE, Cheng P. Natural convection heat transfer from a horizontal cylinder embedded in a porous medium. *International Journal of Heat and Mass Transfer*. 1986;**29**:119-133
- [20] Boomsma K, Poulikakos D, Zwick F. Metal foams as compact high performance heat exchangers. *Mechanics of Materials*. 2003;**35**(12):1161-1176
- [21] Arisetty S, Prasad AK, Advani SG. Metal foams as flow field and gas diffusion layer in direct methanol fuel cells. *Journal of Power Sources*. 2007;**165**(1):49-57
- [22] Calmidi VV, Mahajan RL. Forced convection in high porosity metal foams. *Journal of Heat Transfer*. 2000;**122**(3):557-565
- [23] Brito J, Rodríguez W. Heat transfer characterization of metallic foams. *Industrial and Engineering Chemistry Research*. 2005;**44**(24):9078-9085

- [24] Choi SUS. Enhancing thermal conductivity of fluids with nanoparticle, developments and applications of non-Newtonian flows. *Applied Physics A: Materials Science and Processing*. 1995;**231**(66):99-105
- [25] Lee SP, Choi S, Li S, Eastman JA. Measuring thermal conductivity of fluids containing oxide nanoparticles. *Journal of Heat Transfer*. 1999;**121**(2):280-289
- [26] Li Q, Xuan YM. A preliminary analysis of the intensified thermal-conductivity mechanism of nano-fluids (in Chinese). *Journal of Engineering for Thermal Energy and Power*. 2002;**17**(6):568-571
- [27] Xie HQ, Wang JC, Xi TG, Liu Y, Ai F. Thermal conductivity enhancement of suspensions containing nanosized alumina particles. *Journal of Applied Physics*. 2002;**91**(7):4568-4572
- [28] Eastman JA, Choi SUS, Li S, Yu W, Thompson LJ. Anomalous increased effective thermal conductivities of ethylene glycol-based nanofluids containing copper nanoparticles. *Applied Physics Letters*. 2001;**78**(6):718-720
- [29] Guo SS. The Research on thermophysical Characteristic of Nanofluids (in Chinese). Hangzhou: Zhejiang University; 2006
- [30] Das SK, Putra N, Thiesen P, Raetzl W. Temperature dependence of thermal conductivity enhancement for nanofluids. *Journal of Heat Transfer*. 2003;**125**(4):567-574
- [31] Patel HE, Das SK, Sundararajan T, Nair AS. Thermal conductivities of naked and monolayer protected metal nanoparticle based nanofluids: Manifestation of anomalous enhancement and chemical effects. *Applied Physics Letters*. 2003;**83**(14):2931-2933
- [32] Ebrahimnia-Bajestan E, Moghadam MC, Niazmand H, et al. Experimental and numerical investigation of nanofluids heat transfer characteristics for application in solar heat exchangers. *International Journal of Heat and Mass Transfer*. 2016;**92**(1):1041-1052
- [33] Maxwell JC. *Treatise on Electricity and Magnetism*. Oxford: Clarendon Press; 1873
- [34] Xuan Y, Li Q. Investigation on convective heat transfer and flow features of nanofluids. *Journal of Heat Transfer*. 2003;**125**(1):151-155
- [35] Lee JH, Lee SH, Choi C, Jang S, Choi S. A review of thermal conductivity data, mechanisms and models for nanofluids. *International Journal of Micro-nano Scale Transport*. 2011;**1**(4):269-322
- [36] Corcione M. Empirical correlating equations for predicting the effective thermal conductivity and dynamic viscosity of nanofluids. *Energy Conversion and Management*. 2011;**52**:789-793
- [37] Wang BX, Zhou LP, Peng XF. A fractal model for predicting the effective thermal conductivity of liquid with suspension of nanoparticles. *International Journal of Heat and Mass Transfer*. 2003;**46**(14):2665-2672

- [38] Yu W, Choi SUS. The role of interfacial layers in the enhanced thermal conductivity of nanofluids: A renovated Maxwell model. *Journal of Nanoparticle Research*. 2004;**6**(4): 355-361
- [39] Hadadian M, Samiee S, Ahmadzadeh H, et al. Nanofluids for heat transfer enhancement—A review. *Physical Chemistry Research*. 2013;**1**(1):1-33
- [40] Xue Q, Xu WM. A model of thermal conductivity of nanofluids with interfacial shells. *Materials Chemistry and Physics*. 2005;**90**(2):298-301
- [41] Jang SP, Choi SUS. Role of Brownian motion in the enhanced thermal conductivity of nanofluids. *Applied Physics Letters*. 2004;**84**(21):4316-4318
- [42] Keblinski P, Phillpot SR, Choi SUS, Eastman JA. Mechanisms of heat flow in suspensions of nano-sized particles (nanofluids). *International Journal of Heat and Mass Transfer*. 2002;**45**(4):855-863
- [43] Gao L, Zhou XF. Differential effective medium theory for thermal conductivity in nanofluids. *Physics Letters A*. 2006;**348**(3):355-360
- [44] Xue QZ. Model for thermal conductivity of carbon nanotube-based composites. *Physica B Condensed Matter*. 2005;**368**(1–4):302-307
- [45] Esfe MH, Afrand M, Yan WM, Akbari M. Applicability of artificial neural network and nonlinear regression to predict thermal conductivity modeling of  $\text{Al}_2\text{O}_3$ -water nanofluids using experimental data. *International Journal of Heat and Mass Transfer*. 2016;**66**:246
- [46] Chon CH, Kihm KD, Lee SP, Choi SUS. Empirical correlation finding the role of temperature and particle size for nanofluid ( $\text{Al}_2\text{O}_3$ ) thermal conductivity enhancement. *Applied Physics Letters*. 2005;**87**(15):435
- [47] Khanafer K, Vafai K. A critical synthesis of thermalphysical characteristics of nanofluids. *International Journal of Heat and Mass Transfer*. 2011;**54**(19):4410-4428
- [48] Einstein A. Eineneuebestimmung der moleküldimensionen. *Annalen der Physik*. 1906;**324**: 289-306
- [49] Brinkman HC. The viscosity of concentrated suspensions and solutions. *Journal of Chemical Physics*. 1952;**20**(4):571-581
- [50] Maïga SEB, Palm SJ, Nguyen CT, Roy G, Galanis N. Heat transfer enhancement by using nanofluids in forced convection flows. *International Journal of Heat and Fluid Flow*. 2005;**26**(4):530-546
- [51] Shafahi M, Bianco V, Vafai K, Manca O. Thermal performance of flat-shaped heat pipes using nanofluids. *International Journal of Heat and Mass Transfer*. 2010;**53**(7):1438-1445
- [52] Yang C, Li W, Sano Y, Mochizuki M, Nakayama A. On the anomalous convective heat transfer enhancement in nanofluids: A theoretical answer to the nanofluids controversy. *Journal of Heat Transfer*. 2013;**135**(5):054504



- [53] Xuan Y, Roetzel W. Conceptions for heat transfer correlation of nanofluids. *International Journal of Heat and Mass Transfer*. 2000;**43**(19):3701-3707
- [54] Semenov NS. Mechanism of particle thermophoresis in pure solvents. *Philosophical Magazine*. 2003;**83**(17):2199-2208
- [55] Fu HL. Theoretical Study on Thermophysical Properties and Migration Properties of Nanofluids (in Chinese). Suzhou: Soochow University; 2013
- [56] Corcione M. Heat transfer in nanoparticle suspensions. *International Journal of Heat and Mass Transfer*. 2011;**32**:65-77
- [57] Sakai F, Li W, Nakayama A. A Rigorous Derivation and its Applications of Volume Averaged Transport Equations for Heat Transfer in Nanofluid Saturated Metal Foams. *The International Heat Transfer Conference*; 2014
- [58] Jia T, Wang RX. Convective heat transfer characteristics of MWNTs water-based nanofluid (in Chinese ). *Journal of Refrigeration*. 2015;**36**(1):35-39
- [59] Yang Y, Zhang ZG, Grulke EA, Anderson WB, Wu G. Heat transfer properties of nanoparticle-in-fluid dispersions (nanofluids) in laminar flow. *International Journal of Heat and Mass Transfer*. 2005;**48**(6):1107-1106
- [60] Buongiorno. Convective transport in nanofluids. *Journal of Heat Transfer*. 2006;**128**(3):240-250
- [61] Cheng QF. Experimental Research on Heat Transfer Characteristics of Nanofluids in Foam Metal Heat Pipe (in Chinese). Zhenjiang: Jiangsu University; 2013
- [62] Hajipour M, Dehkordi AM. Mixed-convection flow of  $\text{Al}_2\text{O}_3\text{-H}_2\text{O}$  nanofluid in a channel partially filled with porous metal foam: Experimental and numerical study. *Experimental Thermal and Fluid Science*. 2014;**53**(2):49-56
- [63] Goodarzi M, Safaei MR, Vafai K, Ahmadi G, Dahari M. Investigation of nanofluid mixed convection in a shallow cavity using a two-phase mixture model. *International Journal of Thermal Sciences*. 2014;**75**:204-220
- [64] Mao YB. The heat transfer characteristics of metal foams in nanofluids pool boiling (in Chinese). *Refrigeration*. 2015;**34**(4):6-10
- [65] Nazari M, Ashouri M, Kayhani MH, Tamayol A. Experimental study of convective heat transfer of a nanofluid through a pipe filled with metal foam. *International Journal of Thermal Sciences*. 2015;**83**:33-39
- [66] Matin MH, Pop I. Forced convection heat and mass transfer flow of a nanofluid through a porous channel with a first order chemical reaction on the wall. *International Communications in Heat and Mass Transfer*. 2013;**46**(8):134-141
- [67] Xu HJ, Gong L, Huang SB, Qu ZG, Xu MH. Heat transfer enhancement of nanofluids in metal foams (in Chinese). *Journal of Engineering Thermophysics*. 2014;**35**(8):1586-1590

- [68] Mahdi RA, Mohammed HA, Munisamy KM, Saeid NH. Review of convection heat transfer and fluid flow in porous media with nanofluid. *Renewable and Sustainable Energy Reviews*. 2015;**41**:715-734
- [69] Sivasankaran S, Narrein K. Numerical investigation of two-phase laminar pulsating nanofluid flow in helical microchannel filled with a porous medium. *International Communications in Heat and Mass Transfer*. 2016;**75**:86-91
- [70] Xu HJ, Gong L, Huang SB, Xu MH. Flow and heat transfer characteristics of nanofluid flowing through metal foams. *International Journal of Heat and Mass Transfer*. 2015;**83**(83):399-407
- [71] Sun Q, Pop I. Free convection in a triangle cavity filled with a porous medium saturated with nanofluids with flush mounted heater on the wall. *International Journal of Thermal Sciences*. 2011;**50**(11):5141-5153
- [72] Sherement MA, Pop I, Rahman MM. Three-dimensional natural convection in a porous enclosure filled with a nanofluid using Buongiorno's mathematical model. *International Journal of Heat and Mass Transfer*. 2015;**82**:396-405
- [73] Bhadauria BS, Agarwal S. Convective transport in a nanofluid saturated porous layer with thermal non equilibrium model. *Transport in Porous Media*. 2011;**88**:107-131
- [74] Barber J, Brutin D, Tadrist L. A review on boiling heat transfer enhancement with nanofluids. *Nanoscale Research Letters*. 2011;**6**(1):1-16
- [75] Lee J, Mudawar I. Assessment of the effectiveness of nanofluids for single-phase and two-phase heat transfer in micro-channels. *International Journal of Heat and Mass Transfer*. 2007;**50**(3):452-463
- [76] Kim SJ, Mckrell T, Buongiorno J, Hu LW. Subcooled flow boiling heat transfer of dilute alumina, zinc oxide, and diamond nanofluids at atmospheric pressure. *Nuclear Engineering and Design*. 2010;**240**(5):1186-1194
- [77] Kim SJ, Bang IC, Buongiorno J, Hu LW. Effects of nanoparticle deposition on surface wettability influencing boiling heat transfer in nanofluids. *Applied Physics Letters*. 2006;**89**(15):718
- [78] You SM, Kim JH, Kim KH. Effect of nanoparticles on critical heat flux of water in pool boiling heat transfer. *Applied Physics Letters*. 2003;**83**(16):3374-3376
- [79] Bang IC, Chang SH. Boiling heat transfer performance and phenomena of  $\text{Al}_2\text{O}_3$ -water nanofluids from a plain surface in a pool. *International Journal of Heat and Mass Transfer*. 2005;**48**(12):2407-2419
- [80] Zhu Y, HT H, Ding GL, Peng H, Huang XC, Zhuang DW, et al. Nucleate pool boiling heat transfer characteristics of refrigerant/oil mixture on metal foam covers (in Chinese). *CIESC Journal*. 2011;**62**(2):329-335
- [81] Sundarram SS, Li W. The effect of pore size and porosity on thermal management performance of phase change material infiltrated microcellular metal foams. *Applied Thermal Engineering*. 2014;**64**:147-154

- [82] Zhao CY, Lu W, Tian Y. Heat transfer enhancement for thermal energy storage using metal foams embedded within phase change materials (PCMs). *Solar Energy*. 2010;**84**(8):1402-1412
- [83] Siahpush A, O'Brien J, Crepeau J. Phase change heat transfer enhancement using copper porous foam. *Journal of Heat Transfer*. 2008;**130**(8):318-323
- [84] Hong ST, Herling DR. Effects of surface area density of aluminum foams on thermal conductivity of aluminum foam-phase change material composites. *Advanced Engineering Materials*. 2010;**9**(7):554-557
- [85] Lafdi K, Mesalhy O, Shaikh S. Experimental study on the influence of foam porosity and pore size on the melting of phase change materials. *Applied Physics Letters*. 2007;**102**(8):083549
- [86] Tian Y, Zhao CY. A numerical investigation of heat transfer in phase change materials (PCMs) embedded in porous metals. *Energy*. 2011;**36**(9):5539-5546
- [87] Sundarram SS, Jiang W, Li W. Fabrication of small pore-size nickel foams using Electroless plating of solid-state foamed immiscible polymer blends. *Journal of Manufacturing Science and Engineering*. 2015;**136**(2):021002
- [88] Tao YB, You Y, He YL. Lattice Boltzmann simulation on phase change heat transfer in metal foams/paraffin composite phase change material. *Applied Thermal Engineering*. 2016;**93**:476-485
- [89] Gao D, Tian FB, Chen Z, Zhang D. An improved lattice Boltzmann method for solid-liquid phase change in porous media under local thermal non-equilibrium conditions. *International Journal of Heat and Mass Transfer*. 2017;**110**:58-62
- [90] Wu S, Zhu D, Zhang X, Huang J. Preparation and melting/freezing characteristics of Cu/paraffin Nanofluid as phase-change material (PCM). *Energy and Fuels*. 2010;**24**(3):1894-1898
- [91] Zeng JL, Cao Z, Yang DW, Sun LX, Zhang L. Thermal conductivity enhancement of Ag nanowires on an organic phase change material. *Journal of Thermal Analysis and Calorimetry*. 2010;**101**(1):385-389
- [92] Khodadadi JM, Hosseinizadeh SF. Nanoparticle-enhanced phase change materials (NEPCM) with great potential for improved thermal energy storage. *International Communications in Heat and Mass Transfer*. 2007;**34**(5):534-543
- [93] Guo CX. Application study of nanoparticle-enhanced phase change material in ceiling board. *Advanced Materials Research*. 2011;**150**:723-726
- [94] Wu SY, Wang H, Xiao S, Zhu DS. An investigation of melting/freezing characteristics of nanoparticle-enhanced phase change materials. *Journal of Thermal Analysis and Calorimetry*. 2012;**110**(3):1127-1131

